



Published in final edited form as:

Science. 2013 January 4; 339(6115): 88–91. doi:10.1126/science.1228980.

Para-Aminosalicylic Acid Acts as an Alternative Substrate of Folate Metabolism in *Mycobacterium tuberculosis*

Sumit Chakraborty^{1,2}, Todd Gruber³, Clifton E. Barry III³, Helena I. Boshoff³, and Kyu Y. Rhee^{1,2,*}

¹Department of Medicine, Weill Cornell Medical College, NY, NY, USA

²Department of Microbiology & Immunology, Weill Cornell Medical College, NY, NY, USA

³Tuberculosis Research Section, Laboratory of Clinical Infectious Diseases, National Institute for Allergy and Infectious Diseases, National Institutes of Health, Bethesda, Maryland, USA

Abstract

Folate biosynthesis is an established anti-infective target, and the antifolate *para*-aminosalicylic acid (PAS) was one of the first anti-infectives introduced into clinical practice based on target-based drug discovery. Fifty years later, PAS continues in use for tuberculosis. PAS is assumed to inhibit dihydropteroate synthase (DHPS) in *Mycobacterium tuberculosis* (*M. tuberculosis*) by mimicking the substrate, *p*-aminobenzoate (PABA). However, we found inhibition of DHPS did not inhibit growth of *M. tuberculosis*. Instead, PAS, unlike sulfonamides, served as a replacement substrate for DHPS. Products of PAS metabolism at this and subsequent steps in folate metabolism inhibited those enzymes, competing with their substrates. PAS is thus a prodrug that blocks growth of *M. tuberculosis* when its active forms are generated by enzymes in the pathway that they poison.

Domagk's discovery of the sulfonamide Prontosil, a synthetic prodrug inhibitor of dihydropteroate synthase (DHPS), led to the first commercially available antibiotic and established folate biosynthesis as the first biologically selective target for anti-infectives (Fig. 1A). However, sulfonamides had little activity against *Mycobacterium tuberculosis* (*M. tuberculosis*), the single leading cause of death from bacterial infection (1). Shortly after Waksman's and Schatz's discovery of streptomycin, Lehmann developed *p*-aminosalicylic acid (PAS), a close structural analog of the folate precursor PABA (2), the second drug for tuberculosis (TB). Hitchings subsequently developed antibacterial inhibitors of dihydrofolate reductase and validated a second enzyme of folate metabolism as a therapeutically selective target (3). In parallel, studies of PAS in combination with streptomycin and eventually other anti-TB drugs laid the foundation for modern TB chemotherapy.

Current TB chemotherapy regimens are longer and more complex than for any other bacterial infection, resulting in significant rates of treatment non-compliance, treatment failure, and emergence of multidrug resistant (MDR), extensively drug resistant (XDR) and totally drug resistant (TDR) TB. Given that fresh approaches are needed (4), an improved

*To whom correspondence should be addressed: kyr9001@med.cornell.edu.

Supplementary Materials

www.sciencemag.org

Materials and Methods

Figs. S1, S2, S3, S4, S5

Table S1.

understanding of the mode of action of drugs whose effectiveness has been established in clinical practice seems imperative. Much has been learned from the genetic basis of drug resistance, cell-free assays with candidate target enzymes, measurements of rates of synthesis of the major classes of macromolecules, and transcriptional perturbations and adaptations. However, there have been few, if any, applications of metabolomics to intact bacteria during the pre-lethal phase of drug exposure. Metabolomics is the most direct read-out of the biochemical state of cells with a simultaneous report of uptake and modifications of a drug, and has the potential to reveal the pharmacokinetics and pharmacodynamics that take place within the pathogen.

The presumption that PAS functions as a competitive inhibitor of DHPS, the second enzyme in folate biosynthesis (5), seemed to be supported by the discovery that some PAS resistant strains harbor mutations in the folate consuming enzyme thymidylate synthase A (*thyA*) (6). The puzzle is that PAS is a modest *in vitro* inhibitor of DHPS ($K_i^{app} = 1 \mu\text{M}$), while more potent inhibitors of *M. tuberculosis* DHPS lack activity against intact *M. tuberculosis* (7).

Adapting a filter culture system to support metabolomic profiling of *M. tuberculosis* in response to drug treatment (8), we established that PAS exhibited the same minimal inhibitory concentration (MIC) (1 $\mu\text{g/ml}$) in liquid media and on agar-supported filters, and accumulated in *M. tuberculosis* in a concentration-dependent manner (Fig. 1A, SI Fig. 1). To ensure that a functionally significant proportion of the cell-associated PAS was cytosolic, we monitored intracellular PABA levels as a reporter of PAS binding to DHPS because it is assumed to displace PABA and slow the consumption of PABA. As negative controls, we incubated *M. tuberculosis* with equimolar concentrations of three *in vitro* inhibitors of *M. tuberculosis* DHPS with K_i 's ranging from 10–90 nM, but weak (sulfamethoxazole; MIC= 50 $\mu\text{g/ml}$) or no (sulfanilamide, aminophenylsulfone) whole cell activity and expected to confirm their failure to accumulate in *M. tuberculosis* (7). However, we observed dose-dependent accumulations of all three compounds (Fig. 1A), and of PABA by 18 hours (Fig. 1B), as well as changes in the levels of 154 endogenous metabolites (SI Fig. 2), confirming that they accumulated in *M. tuberculosis* cytosol. The specific patterns of changes in metabolite levels were highly similar for sulfamethoxazole, sulfanilamide and aminophenylsulfone, but less so for PAS.

PAS resulted in a linear dose-dependent accumulation of PABA across the concentration range tested, while the three sulfonamides that are more potent DHPS inhibitors yielded dose-dependent accumulations of PABA that plateaued at levels lower than those achieved by PAS (Fig. 1B). The plateau in PABA accumulation seen with the sulfonamides than with PAS suggested that *M. tuberculosis* may inactivate the sulfonamides, while less effectively disposing of PAS. Indeed, we observed multiple mass species corresponding to inactive biotransformation products of sulfamethoxazole, sulfanilamide and aminophenylsulfone that accumulated in a dose-dependent manner (SI Fig 3, SI Table 1). Since both sulfamethoxazole and aminophenylsulfone resulted in the same degree of PABA accumulation, these results also indicated that DHPS inhibition alone cannot explain the growth inhibitory activity of sulfamethoxazole. Next we focused on the fate of PAS.

Examining the PAS and PABA levels in *M. tuberculosis* over 48 hours, we discovered two distinct but kinetically matched patterns of accumulation (Fig. 2A). PAS accumulation peaked around 6 hours after drug exposure and fell over the next 42 hours. PABA, in contrast, exhibited an early phase of accumulation that slowed by 6 hours and then began to accelerate again until it plateaued after about 18 hours post drug exposure. The dissociation between PAS and PABA levels during the second phase of PABA accumulation suggested that PAS may have undergone enzymatic biotransformation to an additional species also capable of inhibiting DHPS. We sought such products by identifying chromatographically

resolved ion families that were uniquely found in PAS-treated samples and whose abundance increased in a dose-dependent manner. Using authentic chemical standards, we confirmed that PAS underwent sequential mono- and di-methylation at the N4 position (Fig. 2A, SI Table 1) (9). N-mono-methyl PAS was equipotent to PAS in antimycobacterial activity, but N-di-methyl PAS was inactive (10).

We then sought to understand how PAS and N-mono-methyl PAS might affect *M. tuberculosis* folate pathway by identifying biotransformation products corresponding to the sequential turnover of PAS and its N-methyl derivative by *M. tuberculosis* DHPS (FolP1) and dihydrofolate synthase/folyl-polyglutamyl synthase (FolC) (Fig. 2B, SI Fig 4) (11–13). In vitro reactions using the purified recombinant enzymes confirmed that PAS was a kinetically and chemically competent substrate for *M. tuberculosis* FolP1 and could give rise to a dihydrofolate analog (Fig. 2C).

Most reduced folate species, such as dihydrofolate and tetrahydrofolate, exhibit $t_{1/2} < 1$ h (13), rendering it difficult to quantify such PAS-derived folate analogs in *M. tuberculosis*. As a surrogate, we sought to characterize the functional impact of their formation by monitoring the time- and dose-dependent effects of PAS on four folate-dependent pathways in *M. tuberculosis*, the synthesis of glycine, methionine, thymidine triphosphate and purines, which are critical for the synthesis of protein, DNA and RNA. Endogenous levels of dTMP and 5-formamido-1-(5-phospho-D-ribosyl)imidazole-4-carboxamide (FAICAR) were below the limit of detection, but we succeeded in monitoring levels of serine, glycine, homocysteine, methionine, dUMP, and 5-amino-1-(5-phospho-D-ribosyl)imidazole-4-carboxamide (AICAR) as chemically stable, previously validated metabolic surrogates of these pathways (Fig. 3A, SI Fig. 5) (14, 15). Studies in *Escherichia coli* have supported a view of folate biosynthesis in which inhibition at various points in the folate pathway leads to a generalized depletion of folate intermediates and folate-dependent products downstream of the site of inhibition (14). In contrast, treatment with PAS resulted in differential changes in levels of serine, homocysteine, AICAR and dUMP that kinetically followed the accumulation of PABA (Fig. 3A, B). These changes differed from those observed with sulfamethoxazole, sulfanilamide and aminophenylsulfone (Fig. 3A), which inhibit *M. tuberculosis* DHPS, but also caused changes distinct from those reported for *E. coli* treated with an inhibitor of its dihydrofolate reductase (14, 15). Moreover, co-incubation of *M. tuberculosis* with exogenous PABA reversed the changes seen with PAS but did not affect the uptake of PAS or basal levels of the monitored folate-dependent reporters (Fig. 3C). Thus, PAS exerts its antimycobacterial activity through its effects on *M. tuberculosis* folate metabolism downstream of DHPS.

The specific site(s) of PAS action on *M. tuberculosis* folate pathway that result in growth inhibition remain to be elucidated. However, studies of bacterial and human thymidylate synthases, including those of *Mtb*, and AICAR transformylases have reported potent inhibition by dihydrofolate- and methotrexate-related species highly similar to the PAS-derived folate analogs identified here (16–20).

Enzyme inhibition is a cornerstone of rational drug development but observing growth inhibition does not reveal mode of action. Without the ability to monitor directly accumulation of drug with enzyme, biotransformation, enzyme inhibition or other effects, a full understanding of mode of action cannot be achieved.

The metabolomic approach used here showed that PAS, despite its in vitro activity as a competitive inhibitor of DHPS, did not inhibit growth of *M. tuberculosis* by inhibiting DHPS. Sulfonamides that are more potent DHPS inhibitors than PAS but poor antimycobacterial agents do not owe their lack of efficacy to inadequate uptake, as had been

inferred. Instead, they are inactivated by bacterial metabolism and inhibit DHPS only weakly. PAS poisons folate-dependent pathways not only by serving as a replacement substrate for DHPS, but also by the products of that reaction serving as replacement substrates and/or inhibitors of subsequent enzymes.

This discovery revises our understanding of an old drug (PAS) and old target (DHPS) and underscores that catalysis by an enzyme in the target cell or organism, rather than inhibition of that enzyme, can be exploited for drug development.

Supplementary Material

Refer to Web version on PubMed Central for supplementary material.

Acknowledgments

We thank Carl F. Nathan for critical discussions and reading of the manuscript, Richard Lee and Merck Serono for the generous gifts of pure folate intermediates and pterate analogs, a Burroughs Wellcome Career Award in the Biomedical Sciences to KYR, and the Bill and Melinda Gates TB Drug Accelerator Program (OPP1024050) for support. The Department of Microbiology & Immunology acknowledges support from the William Randolph Hearst Foundation. This work was supported in part by the Intramural Research Program of the NIAID, NIH.

References and Notes

1. Raviglione M, et al. *Lancet*. 2012; 379:1902. [PubMed: 22608339]
2. Long, ER. *The Chemistry and Chemotherapy of Tuberculosis*. Baltimore: The Williams & Wilkins Company; 1958.
3. Elion GB, Hitchings GH. *Adv Chemother*. 1965; 2:91. [PubMed: 5319963]
4. Nathan C. *Cell Host Microbe*. 2009; 5:220. [PubMed: 19286131]
5. Rengarajan J, et al. *Mol Microbiol*. 2004; 53:275. [PubMed: 15225321]
6. Mathys V, et al. *Antimicrob Agents Chemother*. 2009; 53:2100. [PubMed: 19237648]
7. Nopponpunth V, Sirawaraporn W, Greene PJ, Santi DV. *J Bacteriol*. 1999; 181:6814. [PubMed: 10542185]
8. de Carvalho LP, et al. *Chem Biol*. 2010; 17:1122. [PubMed: 21035735]
9. Schuessler DL, Parish T. *PLoS One*. 2012; 7:e34471. [PubMed: 22485172]
10. Rosdahl KG. *Svensk Kemisk Tidskrift*. 1948; 60:12.
11. Gengenbacher M, Xu T, Niyomrattanakit P, Spraggon G, Dick T. *FEMS Microbiol Lett*. 2008; 287:128. [PubMed: 18680522]
12. Cole ST, et al. *Nature*. 1998; 393:537. [PubMed: 9634230]
13. Lu W, Kwon YK, Rabinowitz JD. *J Am Soc Mass Spectrom*. 2007; 18:898. [PubMed: 17360194]
14. Kwon YK, Higgins MB, Rabinowitz JD. *ACS Chem Biol*. 2010; 5:787. [PubMed: 20553049]
15. Wei JR, et al. *Proc Natl Acad Sci U S A*. 2011; 108:4176. [PubMed: 21368134]
16. Allegra CJ, Drake JC, Jolivet J, Chabner BA. *Proc Natl Acad Sci U S A*. 1985; 82:4881. [PubMed: 3860829]
17. Allegra CJ, Fine RL, Drake JC, Chabner BA. *J Biol Chem*. 1986; 261:6478. [PubMed: 3700401]
18. Spencer HT, Villafranca JE, Appleman JR. *Biochemistry*. 1997; 36:4212. [PubMed: 9100016]
19. Fivian-Hughes AS, Houghton J, Davis EO. *Microbiology*. 2012; 158:308. [PubMed: 22034487]
20. Hunter JH, Gujjar R, Pang CK, Rathod PK. *PLoS One*. 2008; 3:e2237. [PubMed: 18493582]
21. Brauer MJ, et al. *Proc Natl Acad Sci U S A*. 2006; 103:19302. [PubMed: 17159141]
22. de Carvalho LP, et al. *Chem Biol*. 2010; 17:1122. [PubMed: 21035735]
23. Pesek JJ, Matyska MT, Fischer SM, Sana TR. *J Chromatogr A*. 2008; 1204:48. [PubMed: 18701108]
24. Berglez J, Pilling P, Macreadie I, Fernley RT. *Protein Expr Purif*. 2005; 41:355. [PubMed: 15866722]

25. Young PG, Smith CA, Sun X, Baker EN, Metcalf P. Acta Crystallogr Sect F Struct Biol Cryst Commun. 2006; 62:579.

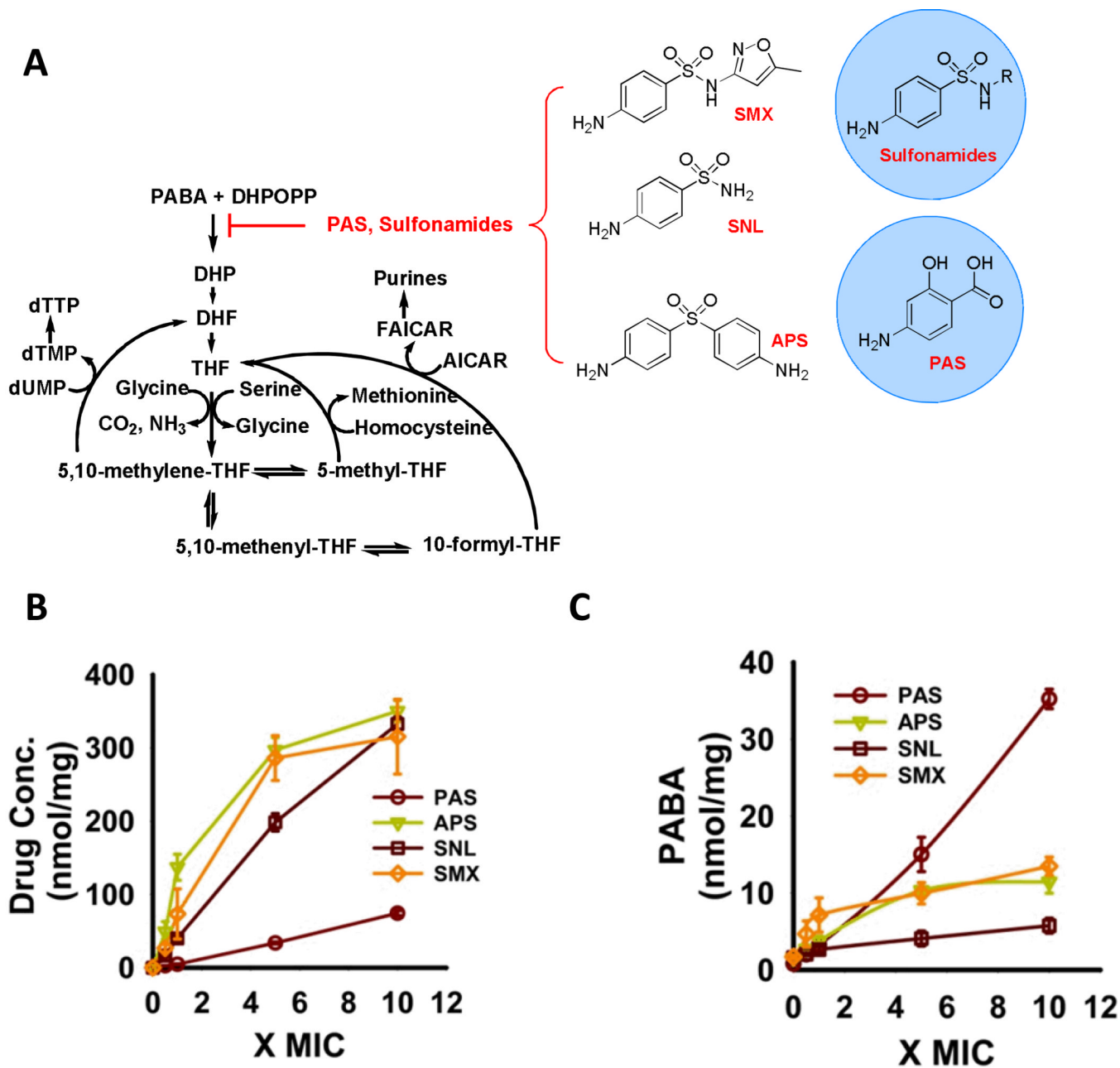


Fig. 1.

[A. Diagram of canonical folate biosynthetic pathway and chemical structures of DHPS inhibitors; MOVED 1A TO SOM] A. Concentration-dependent accumulation of drug within *M. tuberculosis* following incubation of filter-laden *M. tuberculosis* cultures atop drug-impregnated Middlebrook 7H9-based agar media for 18 h. Values on the x-axis denote the relative drug concentration expressed in multiples of the drug's minimum inhibitory concentration (MIC) in plate agar [or, for aminophenylsulfone (APS) and sulfanilamide (SNL)], molar equivalent of sulfamethoxazole (SMX) doses used) determined at day 14. Y-axis values denote relative molar abundance per unit cell biomass as reported by residual protein content of each sample; B. Concentration-dependent accumulation of PABA in *M. tuberculosis* following incubation as in 1B; All values are the average of experimental

triplicates \pm SEM. APS, aminophenylsulfone; MIC, minimal inhibitory concentration; PAS, para-aminosalicylic acid; SNL, sulfanilamide; SMX, sulfamethoxazole.

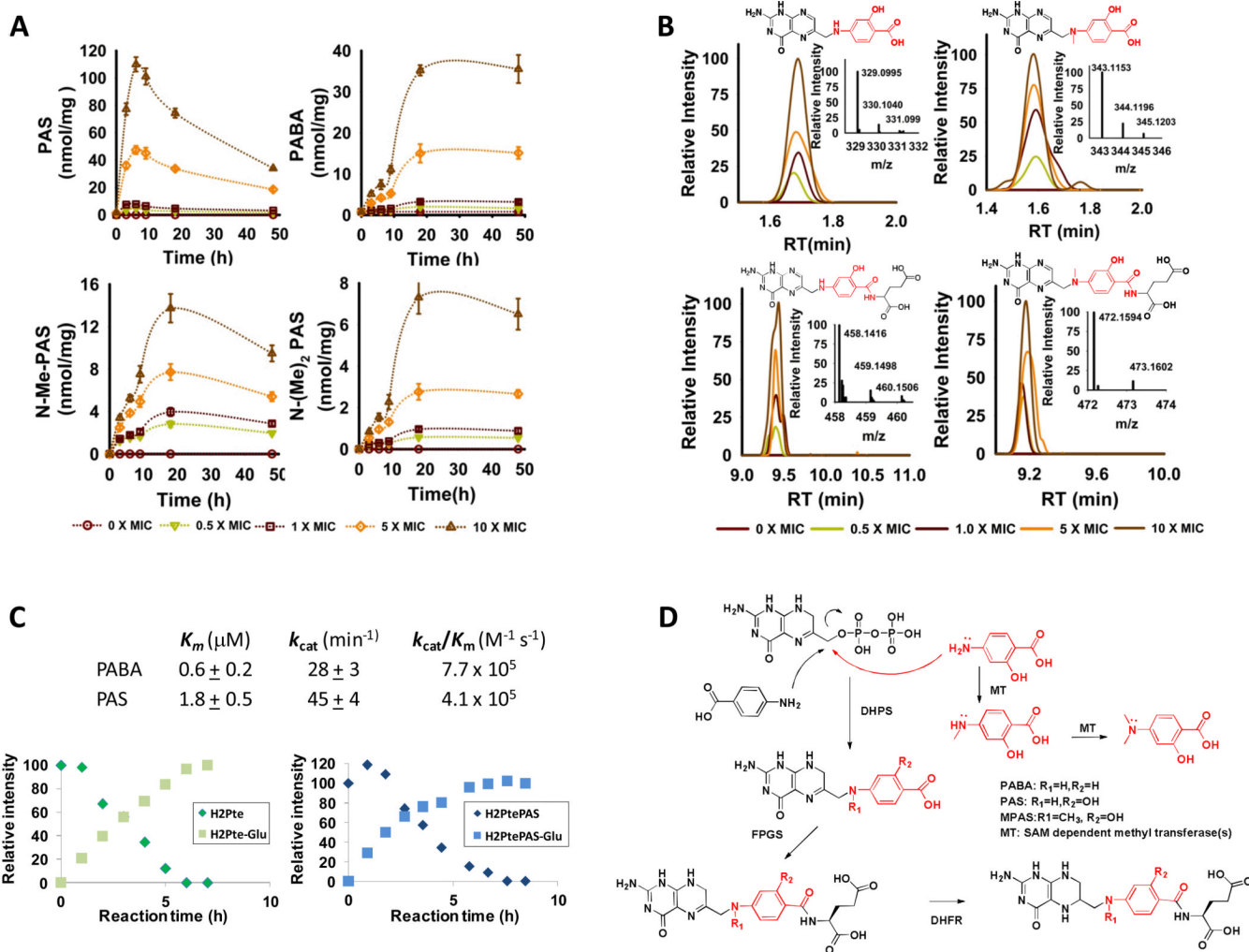


Fig. 2.

A. Time-dependent accumulation of PAS, PABA, *N*-methyl-PAS (*N*-Me-PAS) and *N,N*-dimethyl PAS (*N*-(Me)₂-PAS) in *M. tuberculosis* following incubation with PAS as in Fig. 1C; **B.** Mass spectral profiles displaying concentration-dependent formation of PAS-derived pteroate and folate analogs following exposure of *M. tuberculosis* to PAS for 18 hours; **C.** Chemical and kinetic competence of PABA and PAS as in vitro substrates for purified recombinant *M. tuberculosis* DHPS (top) and FoIC (bottom); **D.** Chemical scheme of PAS-derived biotransformation products. All values are the average of experimental triplicates \pm SEM. RT, retention time; [MOVED 2D TO SOM].

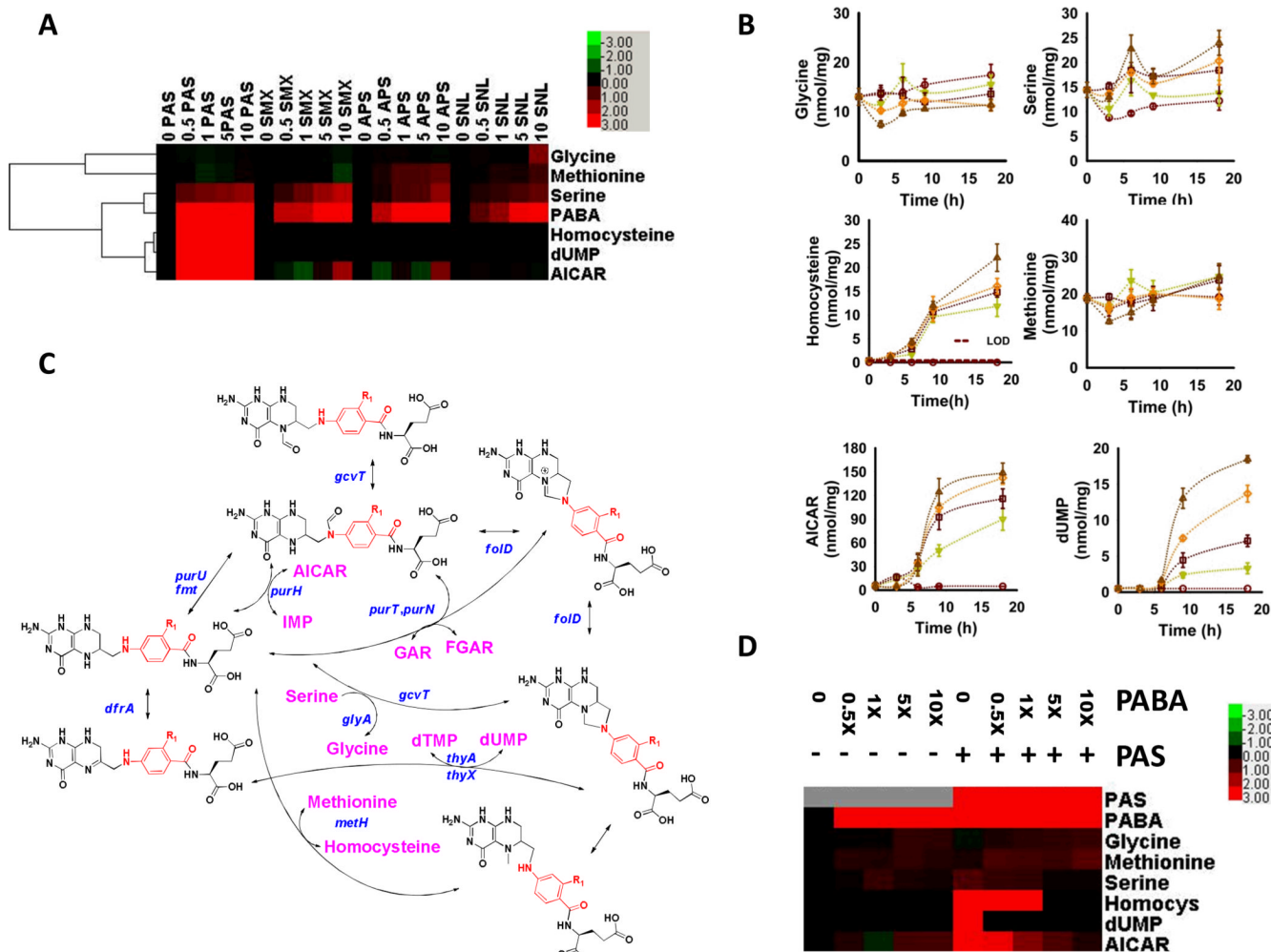


Fig. 3. Heatmap representation of 6 key folate-dependent metabolites in *M. tuberculosis* following treatment with bioequivalent doses of PAS, SMX, APS, or SNL as in **1A**. Numbers denote drug concentration expressed in relation to MIC or, for APS and SNL, molar equivalent of SMX doses used. Color intensities correspond to relative levels of metabolites, and are expressed as the \log_2 -transformed ratio of the normalized signal intensity in drug-treated cells at each concentration to the normalized signal intensity in the drug-free sample, and visually scaled as indicated in upper right inset. Signal intensities were normalized to cell protein biomass at each concentration; **B**. Time-dependent effects of PAS on folate-dependent metabolite levels shown in **3A**. Values on y-axes denote relative molar abundance per unit cell biomass as reported by residual protein content of each sample; [**C**. Metabolic pathway diagram of folate-dependent reactions; MOVED 3C TO SOM] **C**. Heatmap representation demonstrating a time-dependent metabolic rescue of the PAS-induced effects with a 10-fold molar excess of exogenous PABA. All values are the average of experimental triplicates \pm SEM. Labels and abbreviations as in **1B** and **3A**.